Polymer Chemistry

PAPER

View Article Online
View Journal | View Issue

Cite this: *Polym. Chem.*, 2016, **7**, 7086

Biodegradable poly(amidoamine)s with uniform degradation fragments *via* sequence-controlled macromonomers†

M. F. Ebbesen,* C. Gerke, P. Hartwig and L. Hartmann*

Received 29th September 2016,
Accepted 19th October 2016

DOI: 10.1039/c6py01700b

www.rsc.org/polymers

A new and general strategy for the synthesis of high molecular weight, sequence-controlled and selectively degradable poly(amidoamine)s is presented that employs solid-phase synthesis for incorporating degradable linkers at predefined positions within macromonomers. Subsequent molecular weight expansion *via* Cu(I)-catalyzed azide–alkyne cycloaddition (CuAAC)-mediated addition polymerization yields polymers up to an average M_n of 21 kDa. Control of the number and position of degradable linkers within the polymer backbone thus translates into complete and highly selective enzymatic fragmentation down to uniform degradation products. Hence, the control and selectivity of fragmentation now accessible with our strategy can further promote the development of degradable polymers within diagnostic and therapeutic applications.

Introduction

The short half-life of many modern therapeutics such as nucleic acids and peptides in addition to the nonspecific distribution and toxicity of low molecular weight drugs has prompted the development of a broad range of polymer therapeutics that utilize water-soluble polymers for solubilizing, shielding and stabilizing the drug cargo in the bloodstream.[1,2] In addition, high molecular weight therapeutics can provide size-dependent accumulation to certain tissues but are limited to a molecular weight below the renal filtration threshold (20–45 kDa) for proper excretion of non-biodegradable constructs.[3,4]

Over the last decade, this has stimulated an interesting and rapid development towards high molecular weight and biodegradable polymer systems for more efficacious therapeutics that will safely eliminate from the body to ensure biocompatibility.[5,6] Kopeček's group based one strategy on reversible addition–fragmentation chain transfer (RAFT) polymerization of *N*-(2-hydroxypropyl)methacrylamide (HPMA) using a dialkyne chain transfer agent that together with a bis-azido GFLG tetrapeptide linker and *via* Cu(I)-catalyzed azide–alkyne cycloaddition (CuAAC) enabled the formation of an enzymatically degradable multiblock p(HPMA) construct.[7] Pauly *et al.* used Michael addition polymerization for synthesizing terpolymers of ethylene glycol dimethacrylate, ethylenedioxy diethanethiol and one of two different cysteine-terminated tripeptides with either leucine or phenylalanine residues for installing degradability.[8] Being powerful methodologies for generating high molecular weight biodegradable polymer therapeutics, positions and sequences of functionalities (*e.g.* drugs or targeting moieties) incorporated along the polymer backbone are inherently statistically distributed and not necessarily uniform among polymer chains within a single sample. These differences could have important implications for degradation kinetics and *in vivo* distribution.

Degradable polymer therapeutics are metabolized inside the body and thus a proper characterization of both the intact and degraded polymer must be performed for a meaningful assessment of its ADME- (absorption, distribution, metabolism, excretion) and toxicity profile.[9] In this context, polymers that degrade down to uniform fragments might allow a more feasible and complete evaluation of degradation and drug release and thus a more rational design of novel polymer–drug-conjugates.

Previously, our group introduced a strategy for the solid phase synthesis of oligo(amidoamine)s with controlled chain length and monomer sequence that utilizes the automated and stepwise addition of specifically designed functional building blocks.[10] This introduces synthetic control that allows not only for fine-tuning of oligomer properties such as hydrophilicity and molecular weight but also for sequence-defined insertion of a range of functionalities[11,12] such as

Heinrich-Heine-University Düsseldorf, Institute of Organic Chemistry and Macromolecular Chemistry, Universitätsstr. 1, 40225 Düsseldorf, Germany. E-mail: ebbesen@hhu.de, laura.hartmann@hhu.de

†Electronic supplementary information (ESI) available: Materials, synthesis protocols and further analytical data of building blocks, oligomers, polymerizations and polymer degradations. See DOI: 10.1039/c6py01700b

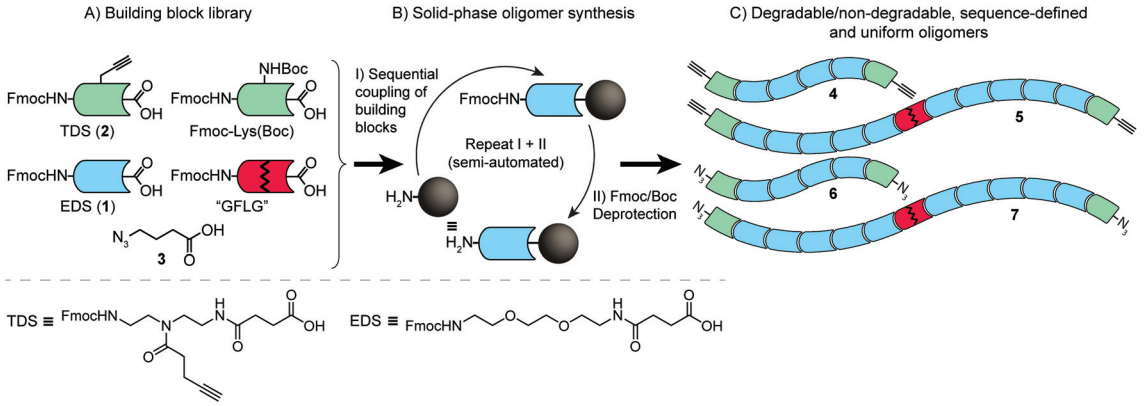

Scheme 1 General strategy for the semi-automated solid-phase synthesis of sequence-defined and degradable/non-degradable oligomers. Building blocks presenting either different functional groups, hydrophilic spacers or composing a degradable peptide sequence (A) were assembled *via* a semi-automated, solid-phase supported process of sequential couplings and deprotections (B) to form a set of four sequence-defined bis-alkyne/bis-azide oligomers with different degradability and length (C).

drugs, ligands for sequence-specific receptor recognition or linkers for degradable oligomer-based structures (Scheme 1).[13–15]

Polymerization of sequence-defined macromonomers has previously been performed using *e.g.* CuAAC-,[16–18] or thiol–ene/yne polymerization[19–21] to obtain sequence-controlled polymers.

Here, we extend our previous sequence-controlled oligo(amidoamine) strategy and demonstrate its application as a tool for the synthesis of a range of poly(amidoamine)s, thereby translating oligomer sequence-control into highly defined polymer structures with selective degradability and improved control of polymer functionality. Furthermore, combining various sequence-defined, degradable and non-degradable α,ω-bis-alkyne/azide oligo(amidoamine)s of different lengths significantly expands the synthetic flexibility with regard to degradable linker density and size of the resulting degradation fragments.

Experimental

Synthesis of building blocks

The preparation of the compound 1-(9*H*-fluoren-9-yl)-3,14-dioxo-2,7,10-trioxa-4,13-diazaheptadecan-17-oic acid, EDS (**1**), previously reported by Ponader *et al.*,[11] was carried out using a trityl protection procedure instead of Boc as adapted from a previously published general method for the synthesis of Fmoc-protected building blocks.[22] See ESI for the synthesis of EDS (**1**) and its precursors (Scheme S1 – ESI†) as well as TDS (**2**) and 4-azidobutanoic acid (**3**).

Solid-phase synthesis (SPS)

Solid-phase reactions (Scheme 1) were performed on a scale of 0.05–0.25 mmol. Coupling of TDS (**2**) (double coupling, 5 eq.), deprotection of Fmoc-L-Lys(Boc)-OH and final oligomer cleavage were carried out manually in syringe-type polypropylene Chromabond columns of 30 mL with a polypropylene frit and cap. The remaining major part of the solid-phase reactions were carried out using an automated Activotec P11 Peptide Synthesizer. Tentagel S RAM resin (loading 0.23 mmol g^{-1}) was used as solid support and was swollen in DCM for 15 min twice prior to synthesis.

General solid-phase synthesis procedure. Fmoc-deprotection was carried out using 25% piperidine in DMF for 20 min and monitored by UV absorption (301 nm) the released fulvene–piperidine adduct. This step was repeated (2–3 times) until the deprotection was complete. Building blocks (EDS **1**, 5 eq.), amino acids (Fmoc-Gly-OH, Fmoc-L-Phe-OH, Fmoc-L-Leu-OH and Fmoc-L-Lys(Boc)-OH, 10 eq.), 4-azidobutanoic acid (10 eq.) and benzotriazol-1-yloxy)tripyrrolidinophosphonium hexafluorophosphate (PyBOP) (1 eq. per building block or amino acid) were placed in vials in the peptide synthesizer. The solids were dissolved in 4 mL of DMF with nitrogen purging. 1 M DIEA solution in DMF (10 or 20 eq.) was added and preactivation was carried out for 3 min in the amino acid vial. Then the coupling mixture was transferred to the resin and agitated carefully for 90 min. The reaction vessel was then emptied and the resin washed with DMF, after which the couplings could be monitored by a colorimetric Kaiser test. After addition of the last residue and Fmoc-deprotection, the oligomer N-terminal was either acetylated using 3 mL of Ac_2O for 5 min (Fig. 1, **4** and **5**) or end-capped (Fig. 1, **6** and **7**) with 4-azidobutanoic acid (**3**) and washed with DMF and DCM.

General procedure for oligomer cleavage from solid support. Final oligomer cleavage from the solid support was performed by adding a cleavage solution (95% TFA, 2.5% triisopropylsilane and 2.5% water 20 mL g^{-1} resin) to the resin and allowing it to react for 90 min. The oligomer-cleavage solution mixture was poured into ice-cold diethyl ether to isolate the oligomer by precipitation. After washing twice with diethyl ether, the residue was dissolved in water and lyophilized to give the final product.

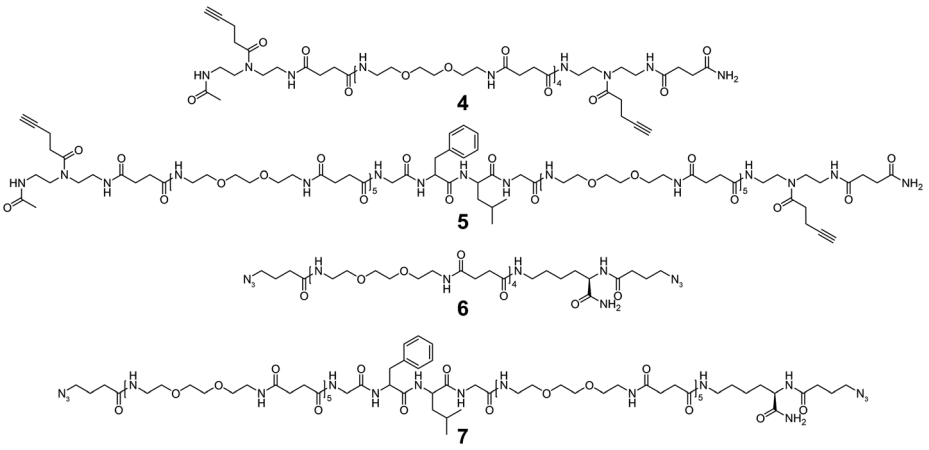

Fig. 1 Set of short/long, degradable/non-degradable oligomers (**4–7**) synthesized on solid phase for subsequent CuAAC-mediated polymerization.

Short non-degradable bis-alkyne oligomer (4). **4** was obtained in 337.2 mg (89.3%). ^{1}H NMR (600 MHz, D_2O) δ 5.46 (s, 1H), 3.71 (s, 1H), 3.68 (s, 16H), 3.62 (t, J = 5.4 Hz, 16H), 3.55–3.47 (m, 8H), 3.44–3.34 (m, 24H), 2.64 (t, J = 6.8 Hz, 4H), 2.58–2.45 (m, 28H), 2.36 (t, J = 2.6 Hz, 2H), 1.99 (s, 1.5H), 1.96 (s, 1.5H). RP-HPLC/MS analysis (0–50% eluent B in 30 min) revealed the oligomer product peak at t_R = 10.77 min and a purity of 91.3%. HRMS (ESI-TOF) m/z: $[M + 2H]^{2+}$ Calcd for $C_{68}H_{117}N_{15}O_{23}$ 755.9218; Found 755.9221.

Long degradable bis-alkyne oligomer (5). **5** was obtained in 273.3 mg (83.7%). ^{1}H NMR (600 MHz, D_2O) δ 7.36 (t, J = 7.4 Hz, 2H), 7.31 (t, J = 7.3 Hz, 1H), 7.27 (d, J = 7.0 Hz, 2H), 4.62 (t, J = 7.6 Hz, 1H), 4.31 (dd, J = 10.0, 4.9 Hz, 1H), 3.90–3.77 (m, 4H), 3.71–3.64 (m, 40H), 3.64–3.57 (m, 40H), 3.54–3.46 (m, 8H), 3.37 (m, 48H), 3.17–3.06 (m, 2H), 2.63 (t, J = 6.8 Hz, 4H), 2.58–2.45 (m, 52H), 2.35 (t, J = 2.6 Hz, 2H), 1.99 (s, 1.5H), 1.95 (s, 1.5H), 1.57 (m, 3H), 0.91 (d, J = 6.3 Hz, 3H), 0.85 (d, J = 6.2 Hz, 3H). RP-HPLC/MS analysis (0–50% eluent B in 30 min), revealed the oligomer product peak at t_R = 15.32 min and a purity of 88.9%. HRMS (ESI-TOF) m/z: $[M + 4H]^{4+}$ Calcd for $C_{147}H_{253}N_{31}O_{51}$ 817.2034; Found 817.2035.

Bis-azido end-functionalization. The bis-azido end-functionality for **6** and **7** was installed through a 4-azidobutanoic acid (**3**)-modification of the oligomer N- and C-terminal. After Fmoc-deprotection of the first residue, Fmoc-L-Lys(Boc)-OH, and addition of **3** to the α-amine, the N-ε Boc group was cleaved using a procedure modified from Han *et al.*[23] (Scheme S2, ESI†). A solution of HCl (4 M) in dioxane was first purged with argon, cooled to 0 °C and then transferred to the resin and mixed for 5 min. The solution was filtered of and the resin was washed once in dioxane before repeating the treatment for 25 min. After washing the resin, first with dioxane and alternating with DCM and IPA (three times each), any remaining HCl was neutralized w/ a solution of DIPEA in DCM (5%, 2 × 10 min) followed by a final wash with DCM and IPA (see ESI† and Results and discussion for further details on the deprotection).

Short non-degradable bis-azido oligomer (6). After coupling the remaining building blocks to the Boc-deprotected oligomer fragment (**6a**, Scheme S2, ESI†), the final oligomer product **6** (71.8 mg, 85.1%) was obtained. ^{1}H NMR (600 MHz, D_2O) δ 4.24 (dd, J = 9.2, 5.2 Hz, 1H), 3.69 (s, 16H), 3.63 (t, J = 5.5 Hz, 16H), 3.43–3.35 (m, 20H), 3.18 (t, J = 6.8 Hz, 2H), 2.58–2.49 (m, 16H), 2.41 (td, J = 7.3, 2.5 Hz, 2H), 2.36 (t, J = 7.4 Hz, 2H), 1.93–1.86 (m, 4H), 1.85–1.78 (m, 1H), 1.72 (dtd, J = 14.2, 9.5, 5.0 Hz, 1H), 1.57–1.48 (m, 2H), 1.47–1.33 (m, 2H). RP-HPLC/MS analysis (0–50% eluent B in 30 min), revealed the oligomer product peak at t_R = 13.09 min and a purity of 92.6%. HRMS (ESI-TOF) m/z: $[M + 2H]^{2+}$ Calcd for $C_{54}H_{99}N_{17}O_{19}$ 644.8646; Found 644.8648.

Long degradable bis-azido oligomer (7). The crude oligomer product was cleaved from the resin in a purity of 75% and was therefore purified *via* preparative RP-HPLC to obtain oligomer **7** (430.2 mg, 70.7%). ^{1}H NMR (600 MHz, D_2O) δ 7.38 (t, J = 7.4 Hz, 2H), 7.33 (t, J = 7.3 Hz, 1H), 7.28 (d, J = 7.0 Hz, 2H), 4.64 (t, J = 7.6 Hz, 1H), 4.32 (dd, J = 9.9, 4.8 Hz, 1H), 4.24 (dd, J = 9.2, 5.2 Hz, 1H), 3.91–3.80 (m, 4H), 3.70–3.66 (m, 40H), 3.65–3.59 (m, 40H), 3.47–3.34 (m, 44H), 3.18 (t, J = 6.9 Hz, 2H), 3.17–3.06 (m, 2H), 2.63–2.48 (m, 40H), 2.41 (td, J = 7.3, 2.3 Hz, 2H), 2.36 (t, J = 7.3 Hz, 2H), 1.93–1.85 (m, 4H), 1.85–1.78 (m, 1H), 1.72 (dtd, J = 14.2, 9.5, 5.0 Hz, 1H), 1.67–1.48 (m, 5H), 1.48–1.31 (m, 2H), 0.93 (d, J = 6.1 Hz, 3H), 0.87 (d, J = 6.0 Hz, 3H). RP-HPLC/MS analysis (0–50% eluent B in 30 min), revealed the oligomer product peak a t_R = 16.92 min and a purity of 99.8%. HRMS (ESI-TOF) m/z: $[M + 4H]^{4+}$ Calcd for $C_{133}H_{235}N_{33}O_{47}$ 761.6748; Found 761.6759.

Copper(I)-catalyzed azide–alkyne cycloaddition (CuAAC)-mediated oligomer polymerization

The CuAAC mediated polymerization of azide- and alkyne modified oligomers, **4–7**, and 1,11-bis-azido-PEG3 (**L**) (Scheme 2) was performed on a 4 μmol scale. Various reaction parameters were tested (Tables 1 and S1†) with the optimal conditions described here. Oligomers were dissolved in water (50 mmol L^{-1}), mixed according to the desired oligomer composition (at 1 : 1 molar eq.) and freeze-dried in glass HPLC vials. Subsequently, solid sodium ascorbate (4 eq.) and a

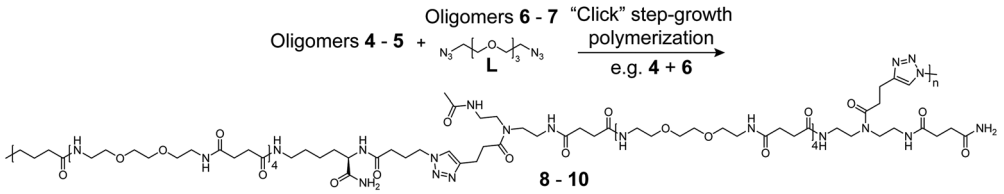

Scheme 2 CuAAC mediated polymerization of matching bis-alkyne (**4–5**) and bis-azide (**6–7** + **L**) oligomer pairs. Polymerization of **4** and **6** are here shown as example. Polymerization of oligomer **4** and the linker 1,11-diazido-PEG3 (**L**) was performed for initial reaction optimization (see ESI†).

Table 1 Polymerization parameters for polymers **8–12** from biz-alkyne (**4–5**) and bis-azide (**6–7**) oligomers and GPC characterization

#	Bis-C≡CH oligomer	Bis-N_3 oligomer	DMSO/DMF/H_2O	Catalyst	Rx. [h]	M_n [a] [kDa]	$Đ_M$ [b]	X_n [c]
8	**4** (1.51 kDa)	**6** (1.29 kDa)	0/10/0	$CuSO_4$	4	1.7	1.6	1.2
9	—	—	0/9/1	—	—	20.8	1.5	14.8
10	—	—	0/7/3	—	—	16.9	1.6	12.0
11	**5** (3.27 kDa)	**6** (1.29 kDa)	0/9/1	$CuSO_4$	4	17.3	2.0	7.6
12	**5** (3.27 kDa)	**7** (3.04 kDa)	—	—	—	14.1	2.3	4.5

[a] Number averaged molecular mass measured using GPC-MALS as described in the ESI. [b] Molecular mass distribution (M_w/M_n). [c] Number-average degree of polymerization.

deoxygenated solvent mixture (DMF/water 9/1, purged with Ar for at least 10 min) containing the copper catalyst ($CuSO_4$ or CuBr, 0.4 eq.) was added to an oligomer concentration of 100 mg mL^{-1} and the vial was capped and mixed thoroughly. Then the vial was shaken (1500 rpm) for 4 h at 25 °C. Hereafter the reaction mixture was diluted with a 1.3 mL aq. solution of sodium diethyldithiocarbamate (10 eq. to the Cu catalyst), stirred 20 min and filtrated through 0.2 um syringe filters to remove the Cu-diethyldithiocarbamate precipitate.[24] Complete removal of Cu (to below 0.0005 wt%) was verified by Atomic Absorption Spectroscopy. After extensive dialysis (Vivaspin 2 concentrators, MWCO 2 kDa) against Millipore water and freeze-drying, the resulting polymers were obtained as faint yellow solids in yields between 80% and 90% and analysed by gel permeation chromatography-multi angle light scattering (GPC-MALS) and ^{1}H-NMR (Fig. 2, Tables 1, S1 and Fig. S18, 19 ESI†).

Enzyme mediated polymer degradation

The enzyme-mediated degradation of the polymers (Fig. 3 and 4) was performed following a procedure modified from Luo *et al.*[25] Papain was used as a model enzyme for the degradation. Stock papain enzyme purity was determined by UV at 280 nm from a 1 mg mL^{-1} enzyme solution in McIlvaine's buffer (50 mM sodium citrate, 100 mM NaH_2PO_4, 2 mM EDTA, pH 6.0) using the extinction coefficient 1% = 25.[26] Equal volumes of glutathione solution (10 mM) and papain stock solution (16 μM) in McIlvaine's buffer were mixed and preincubated for 5 min at 37 °C. Finally, the enzymatic degradation was performed at 37 °C with a polymer concentration of 3 mg mL^{-1} and papain concentration of 8 μM. Aliquots of 350 μL were taken out at predetermined time points, snap-frozen in filter vials (Mini-UniPrep, 0.2 μm porosity) and stored at −20 °C. GPC analysis was performed after thawing (5 min, 37 °C) and filtration of the individual samples (Fig. 3). MALDI-TOF mass analysis was performed before and 24 h after the enzyme treatment (Fig. S20–22 and Table S2, 3†).

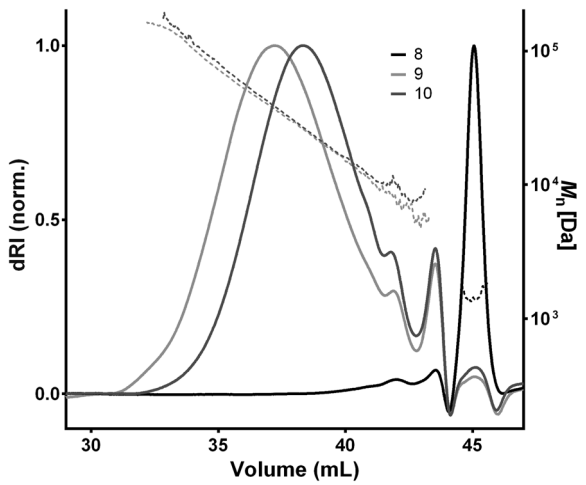

Fig. 2 GPC elugrams of polymerizations **8–10** performed in three different reaction solvent compositions (Table 1). The highest molecular weight polymer (**9**) were observed for solvent compositions DMF/H_2O 9/1 with essentially only monomeric species (eluting at 45 mL) shown for DMF only (**8**). Full lines traces the dRI signal and dashed lines traces the molecular mass.

Results and discussion

The overall synthetic strategy is based on the solid-phase-mediated introduction of enzymatically degradable sequences within a set of uniform oligomers synthesized from specially

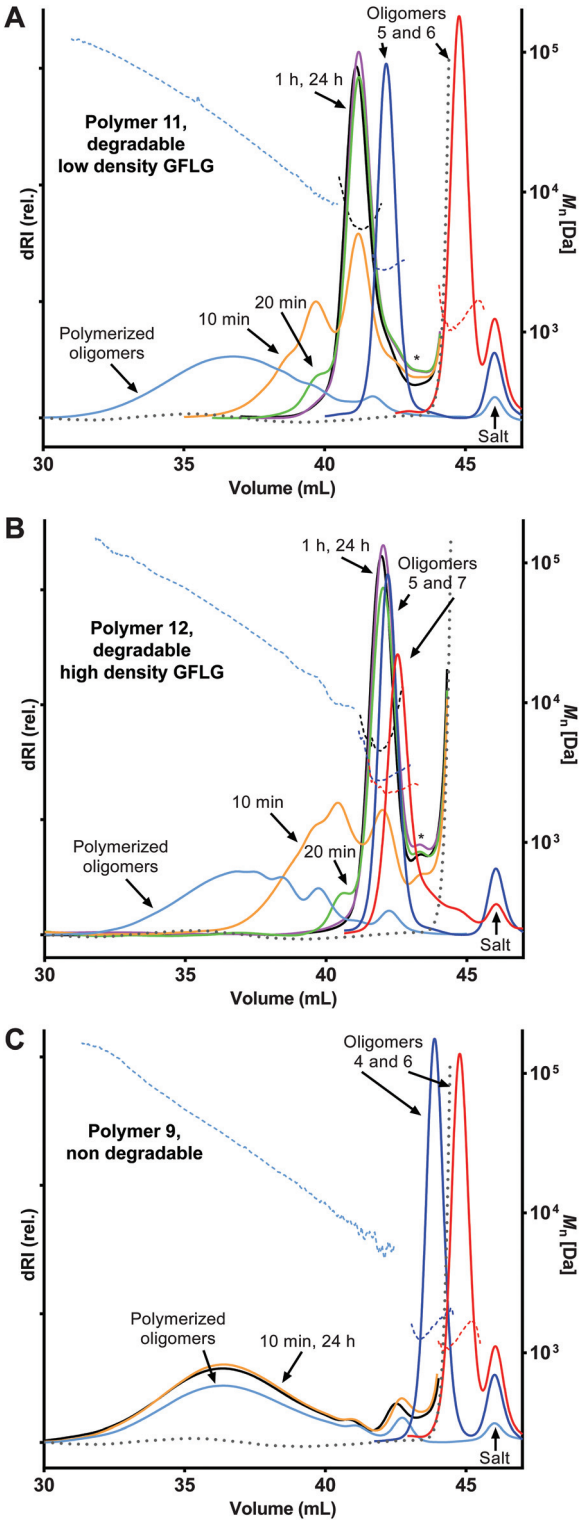

Fig. 3 GPC profiles at various time points of degradable- (A and B) and non-degradable (C) sequence-defined polymers treated with papain (8.0 μM, within a pH 6.0 McIlvaine's buffer at 37 °C). * Denotes smaller degradation fragments derived from polymer terminals. The initial oligomer constituents (**4**–**7**) are also shown for comparison. Full lines traces the dRI signal and dashed lines traces the molecular mass. The stippled grey trace denotes a "blank" run with the McIlvaine's buffer used for the papain treatment.

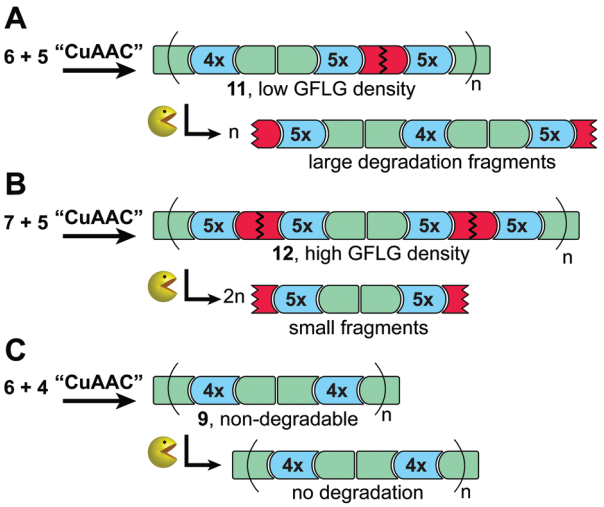

Fig. 4 The combination and polymerization of oligomer macromonomers (**4**–**7**) of various size and degradability translates oligomer sequence-control into highly defined precision-polymers (**11**, **12** and **9**) that selectively degrades down to fragments of uniform sizes equal to the average size of the degradable oligomers and any non-degradable oligomers within the polymer.

designed building blocks (Scheme 1). Subsequent molecular weight expansion through CuAAC-mediated addition polymerization (Scheme 2) leads to the sequence-controlled and selectively degradable precision polymers.

Building blocks

Besides being compatible with standard Fmoc solid-phase polyamide synthesis (Scheme 1A), the applied building blocks are individually designed and/or selected towards a particular purpose such as attachment of ligands, drugs or for degradability.[11,14] In this study, the CuAAC coupling was selected for the final oligomer addition polymerization (Scheme 2) due to its high coupling efficiency but also due to orthogonality towards the coupling chemistry used with solid phase oligomer synthesis.[27,28] Therefore, in addition to a free carboxylic acid and an Fmoc-protected amine group, important features of the applied building blocks were alkyne and azide functionalities. These were introduced *via* the alkyne-functional building block 1-(fluorenyl)-3,11-dioxo-7-(pent-4-ynoyl)-2-oxa-4,7,10-triazatetradecan-14-oic acid (TDS, **2**), previously synthesized in our group,[11,22] and *via* on-resin azido-functionalization of terminal building blocks (Schemes 1 and S2, ESI†). A second building block based on 2,2′(ethylenedioxy)bis(ethylamine) (EDS, **1**) was synthesized *via* a Trt intermediate updating the previous synthetic route *via* a Boc intermediate and then ubiquitously utilized for conferring hydrophilicity and flexibility to the final polymer backbone (see ESI for synthesis of TDS and EDS (Scheme S1†)).

Previously, biodegradability has been installed within sequence-defined oligomers using disulfide containing building blocks as introduced by Hartmann *et al.*[14] The present strategy utilizes a GFLG tetrapeptidyl linker known from work

by Kopeček and Duncan[29] which is seamlessly introduced into our solid-phase oligo(amidoamine) synthesis *via* sequential addition of its Fmoc-protected amino acid components to ultimately generate sequence-defined and selectively degradable precision polymers.

Synthesis of selectively degradable uniform oligomers

Four different oligomer structures varying in length, end group functionality and degradability (Fig. 1) were synthesized using optimized PyBOP-mediated activation chemistry and deprotection protocols that enabled the synthesis of sequence-controlled oligomers in high purity (Scheme 1).[22] Coupling of TDS, deprotection of Fmoc-L-Lys(Boc)-OH and final oligomer cleavage were carried out manually in syringe-type polypropylene columns while the remaining major part of the solid-phase reactions could be carried out on an automated peptide synthesizer. After acetylation of the free N-terminal group and cleavage from the resin, oligomer **4** and **5** were precipitated in diethyl ether and lyophilized from aqueous solution. No further purification was performed.

The azido-equivalents of oligomer **4** and **5** (**6** and **7**, Fig. 1) were targeted *via* functionalizing oligomer terminal residues with 4-azidobutanoic acid (**3**). This required a selective deprotection of a C-terminal amine group that was initially pursued *via* orthogonal deprotection of a Fmoc-L-Lys(Aloc)-OH residue but without achieving the deprotected product in the desired purity. A Boc deprotection strategy was therefore employed using Fmoc-L-Lys(Boc)-OH as the initial C-terminal building block. After initial Fmoc deprotection and capping of the lysine α-amine with **3**, Boc deprotection was performed following a procedure from Han *et al.*[23] using a cold 4 M solution of HCl in dioxane (see ESI† for further details). This procedure allowed the continued and automated addition of the residual building blocks and after capping the N-terminus with **3**, the final oligomer products **6** and **7** could be isolated in a similar way to **4** and **5**. Oligomer **7** was cleaved from the resin in 75% crude purity and was therefore purified *via* preparative RP-HPLC.

Analysis by RP-HPLC/MS (0–50% eluent B in 30 min, UV detection at 214 nm) and ESI-HRMS revealed uniform oligomer products with the expected mass-to-charge (m/z) ratios and purities of 91% (**4**), 89% (**5**), 93% (**6**) and >99% (**7**), respectively. The slightly higher crude purities of **4** and **6** reflect the lower number of couplings required for these oligomers and the absence of the more hydrophobic Phe and Lys residues, which often lead to more difficult couplings due to aggregation.[30] NMR analysis confirmed the desired oligomer structure (see ESI, Fig. S4–17,† for detailed analytical data).

In summary, four uniform, sequence-defined and selectively degradable/non-degradable oligomers (**4–7**, Fig. 1) with different lengths and end-group functionalities were obtained and next applied for CuAAC-mediated addition polymerization to create selectively degradable polymers.

Polymerization

As the solid-phase synthesis of oligo(amidoamine)s is typically restricted to molecular weights below ~5 kDa,[30] further expansion is necessary for providing certain size-dependent properties such as enhanced biodistribution to the final therapeutic construct.[4] CuAAC-mediated addition polymerization is well-known with macromonomers composed especially from atom transfer radical polymerization (ATRP) synthesized polymers[31] and polymer–peptide mixtures,[25] whereas only a few studies describe all-peptide macromonomers.[17,18]

In this work, four sequence-defined, bis-alkyne and bis-azido terminated oligomers (**4–7**) were synthesized and applied as homobifunctional macromonomers for CuAAC-mediated addition polymerization (Scheme 2). For initial testing purposes, a macromonomer system comprised of 1,11-bis-azido-PEG3 (**L**), and an oligomer (**4**) was used (Table S1†) that was later replaced by oligomer macromonomers **4** and **6** (Table 1, Fig. 2) to obtain the desired products. In general, special care was taken to add a 1 : 1 stoichiometric mixture of the selected oligomers to optimize polymerization conversion and, moreover, the oligomer/linker concentration was kept as high as possible to increase the reactive group concentration for decreasing the probability for intramolecular ring formation.

The influence of the reaction solvent, reaction time and catalyst type was then tested for optimizing the polymerization reaction with regard to the degree of polymerization (X_n) that was measured *via* GPC analysis. No significant differences were found for reaction times in the range 2 to 24 h (Table S1†). CuBr is a commonly used CuAAC catalyst in DMF due to suitable solubility.[25] Here, a direct comparison to $CuSO_4$ catalysis in various DMF/water ratios (Table S1†), however, showed a higher X_n for $CuSO_4$ (X_n = 9.3) compared to CuBr (X_n = 6.7). $CuSO_4$ was therefore used for subsequent polymerizations. A comparison of polymerizations performed under various solvent conditions (Table 1, **8–10** and Table S1,† **16–20**) illustrated the benefit of fine-tuning reaction solvent parameters with neither water nor DMF alone providing optimal results. Water has been well-recognized for being a good solvent for supporting Cu(I)-acetylides and for the Cu-ligand exchange[32] and also seemed a crucial component of the solvent mixture in this study with a X_n of 10.6 for a DMF/water 9/1 mixture and $CuSO_4$ as Cu(I) source. More than 10% water, however, led to decreased X_n, possibly due to alkyne water addition hereby forming an unreactive ketone. Overall, the best reaction parameters were determined to be a $CuSO_4$/NaAsc. mixture (0.4/4 eq.) in a deoxygenated DMF/water 9/1 with 4 h reaction time at 25 °C. The optimized conditions showed a low level of remaining oligomer *via* GPC analysis (Fig. 2) and ^{1}H-NMR analysis (Fig. S19 – ESI†) showed full consumption of the alkyne proton at 2.36 ppm and confirmed the overall polymer structure.

As shown in the literature, the degree of polymerization (X_n) obtained from macromonomer addition polymerization depends on the monomer size due to a lower effective concentration of the reactive end-groups for larger monomers with a typical X_n around 15 for monomers >1 kDa and higher X_n for lower molecular weight monomers.[25,33] Despite the larger average monomer size, polymerization of oligomers **4** and **6**

showed a higher maximal X_n of 14.8 (**9**, Table 1, Fig. 2) compared to the test system (**L** + **4**, Table S1 – ESI†) that could probably be ascribed to high oligomer end-group purities. The X_n and $Đ_M$ values obtained correlate well with previous examples of CuAAC-mediated macromonomer addition polymerization (before fractionation) with $Đ_M$ between ~1.5 and 2 and maximal X_n values in the range of ~13–16.[17,18,25,31] Refinement of the synthesis by preparative fractionation should lead to polymers of higher X_n with lower $Đ_M$ values.[25] Subsequently, different sets of degradable and non-degradable oligomers were selected and copolymerized to obtain polymers with pre-determined densities of cleavage sites. Comprised of larger oligomers, these polymers (**11–12**) displayed a somewhat lower X_n (Table 1) due to the lower reactive group concentration.

In summary, the CuAAC-mediated polymerization of selected combinations of sequence-defined and degradable/non-degradable azide/alkyne terminated macromonomers enabled the synthesis of precision polymers with selective degradation profiles. A set of three selectively degradable/non-degradable polymers were then subjected to enzymatic degradation for demonstrating their controlled degradation down to uniform fragments.

Enzyme-mediated polymer degradation

The enzyme-cleavable tetrapeptide sequence, GFLG, is not a natural substrate for serum enzymes, which ensures stability in serum but prompt degradation when internalized into endocytic vessels containing the cysteine protease cathepsin-B that recognizes and cleaves it.[29,34] Enzymatically degradable polymers are, therefore, unique in terms of the high selectivity between enzyme and substrate that allows for spatially (enzyme location) controlled degradation,[35,36] but, as shown in this work, potentially also structural (polymer) degradation control by exact positioning of the degradable peptide sequence within the polymer backbone.

Polymer degradation was investigated using a low-cost alternative to cathepsin B. Papain is an enzyme in the same group of cysteine proteases and has a substrate specificity similar to cathepsin B.[34] The selectively degradable precision polymers comprising GFLG linkers (**11**, **12**) (Fig. 4A and B) and non-degradable polymers without GFLG as control (**9**) (Fig. 4C) were incubated with 8.0 μM papain under slightly acidic and reducing conditions (pH 6 and 37 °C) up to 24 h leading to rapid onset of polymer degradation with complete degradation within 1 h as determined by GPC analysis (Fig. 3). This was faster than a previous similar study based on degradable multiblock polyHPMA[25] which could potentially be attributed to a higher GFLG density and less steric hindrance for the lower M_n structures reported in our study. The presence of low X_n populations (monomer, dimer, *etc.*) for **11** and **12** entails a higher amount of polymer terminals. Cleavage of terminal GFLG linkers from these polymers thus lead to an observable amount of smaller degradation fragments derived from the polymer terminals (Fig. 3A and B). The presence of these smaller fragments should be significantly reduced in the next generation of materials with optimized and longer polymer chains lowering the relative amount of polymer terminals.

Uniform degradation fragments were obtained with sizes depending on the individual oligomer combinations in terms of size and degradability (Fig. 3 and 4). MALDI-MS analysis was performed (Fig. S20, 21 and Table S2, 3 – ESI†) and confirmed complete polymer degradation down to a very narrow range of fragments corresponding to the average size of the degradable oligomers and any non-degradable oligomers within the polymer (4.2–4.9 kDa and 2.8–3.4 kDa for polymer **11** and **12**, respectively, Table S2†). Likewise, MALDI-MS analysis in combination with our sequence-defined polymers also provided a qualitative view on the enzyme peptidase activity towards GFLG. Papain is considered an endopeptidase and cleaves amide bonds within the GFLG sequence except in the sterically crowded site between Phe and Leu residues.[37] Interestingly, from our study we found that papain also degraded amide bonds between synthetic EDS building blocks and Gly amino acid residues (see ESI, Fig. S21–22 and Table S3†). This might contribute to further development of enzyme-degradable polymer linkers and opens up further potential *e.g.* for an all-artificial enzymatically degradable linker synthesized from our present building block library.

No significant changes were observed for the GPC traces between 1 h and 24 h (Fig. 3A and B) that indicates no further degradation of the fragments within this timeframe. The stability of the non-degradable polymers was confirmed in a similar manner (Fig. 3C) that supported the observed degradation to be mediated by the GFLG linker. A low degree of non-enzymatic hydrolysis has previously been reported for the GFLG linker[38] and thus further studies on the long-term stability of the degradable and non-degradable polymers are currently ongoing.

The resulting sequence-controlled and selectively degradable precision poly(amidoamines) represent a promising class of materials not previously used within polymer therapeutics. Similar to previous reported biodegradable polymers,[25] the design allows efficient enzymatic degradation and with the additional possibilities for controlling the size of polymer degradation fragments, this strategy could ultimately be of great importance *e.g.* for the development new degradable polymers with a more predictive release and body clearance profile.

Conclusions

The purpose of this study was to introduce a new approach for the synthesis of sequence-defined and biodegradable polymers for further enhancing the spatial and structural controlled fragmentation of polymers. This was demonstrated *via* the solid-phase-supported synthesis of a set of sequence-defined azide- and alkyne terminated oligomers containing enzymatically degradable linkers at predefined positions. Subsequent CuAAC-mediated addition polymerization expanded the average molecular weight up to 15 times (M_n 21 kDa). Finally,

complete and efficient enzymatic degradation down to a narrow range of uniform degradation products validated the approach for the synthesis of selectively degradable precision polymers. The envisioned benefits include highly defined degradation products and a flexible yet more consistent synthesis without inherent heterogeneities in terms of positions and sequences of polymer functionalities that has potential to further promote the use of polymeric therapeutics.

Acknowledgements

M. F. E. thanks the Danish Council for Independent Research for support through the grant DFF – 4005-00023. L. H. thanks the Boehringer-Ingelheim-Stiftung for support through the "Perspektivenprogramm Plus-3". Moreover, the authors are grateful to Assoc. Prof. Nicole Snyder (Davidson College, North Carolina) for fruitful discussions.

References

1 R. Duncan and M. J. Vicent, *Adv. Drug Delivery Rev.*, 2013, **65**, 60–70.
2 M. Ebbesen, K. Bienk, B. Deleuran and K. Howard, *Molecular and Cellular Therapies*, 2014, **2**, 29.
3 D. G. Rudmann, J. T. Alston, J. C. Hanson and S. Heidel, *Toxicol. Pathol.*, 2013, **41**, 970–983.
4 J. G. Shiah, M. Dvořák, P. Kopečková, Y. Sun, C. M. Peterson and J. Kopeček, *Eur. J. Cancer*, 2001, **37**, 131–139.
5 A. V. Yurkovetskiy and R. J. Fram, *Adv. Drug Delivery Rev.*, 2009, **61**, 1193–1202.
6 J. W. Singer, *J. Controlled Release*, 2005, **109**, 120–126.
7 R. Zhang, K. Luo, J. Yang, M. Sima, Y. Sun, M. M. Janát-Amsbury and J. Kopeček, *J. Controlled Release*, 2013, **166**, 66–74.
8 A. C. Pauly and F. di Lena, *Polymer*, 2015, **72**, 378–381.
9 E. Markovsky, H. Baabur-Cohen, A. Eldar-Boock, L. Omer, G. Tiram, S. Ferber, P. Ofek, D. Polyak, A. Scomparin and R. Satchi-Fainaro, *J. Controlled Release*, 2012, **161**, 446–460.
10 L. Hartmann and H. G. Börner, *Adv. Mater.*, 2009, **21**, 3425–3431.
11 D. Ponader, F. Wojcik, F. Beceren-Braun, J. Dernedde and L. Hartmann, *Biomacromolecules*, 2012, **13**, 1845–1852.
12 F. Wojcik, A. G. O'Brien, S. Götze, P. H. Seeberger and L. Hartmann, *Chem. – Eur. J.*, 2013, **19**, 3090–3098.
13 D. Ponader, P. Maffre, J. Aretz, D. Pussak, N. M. Ninnemann, S. Schmidt, P. H. Seeberger, C. Rademacher, G. U. Nienhaus and L. Hartmann, *J. Am. Chem. Soc.*, 2014, **136**, 2008–2016.
14 L. Hartmann, S. Häfele, R. Peschka-Süss, M. Antonietti and H. G. Börner, *Macromolecules*, 2007, **40**, 7771–7776.
15 J.-F. Lutz, M. Ouchi, D. R. Liu and M. Sawamoto, *Science*, 2013, **341**, 1238149.
16 M.-A. Berthet, Z. Zarafshani, S. Pfeifer and J.-F. Lutz, *Macromolecules*, 2010, **43**, 44–50.
17 T.-B. Yu, J. Z. Bai and Z. Guan, *Angew. Chem., Int. Ed.*, 2009, **48**, 1097–1101.
18 S. van der Wal, C. J. Capicciotti, S. Rontogianni, R. N. Ben and R. M. J. Liskamp, *MedChemComm*, 2014, **5**, 1159–1165.
19 F. Driessen, F. E. Du Prez and P. Espeel, *ACS Macro Lett.*, 2015, **4**, 616–619.
20 W. Xi, S. Pattanayak, C. Wang, B. Fairbanks, T. Gong, J. Wagner, C. J. Kloxin and C. N. Bowman, *Angew. Chem., Int. Ed.*, 2015, **54**, 14462–14467.
21 J. Han, Y. Zheng, B. Zhao, S. Li, Y. Zhang and C. Gao, *Sci. Rep.*, 2014, **4**, 4387.
22 F. Wojcik, S. Mosca and L. Hartmann, *J. Org. Chem.*, 2012, **77**, 4226–4234.
23 G. Han, M. Tamaki and V. J. Hruby, *J. Pept. Res.*, 2001, **58**, 338–341.
24 B. J. Strawter, *Canada Pat.*, CA1186076, 1985.
25 K. Luo, J. Yang, P. Kopečková and J. Kopeček, *Macromolecules*, 2011, **44**, 2481–2488.
26 A. N. Glazer and E. L. Smith, *J. Biol. Chem.*, 1961, **236**, 2948–2951.
27 W. H. Binder and R. Sachsenhofer, *Macromol. Rapid Commun.*, 2008, **29**, 952–981.
28 V. V. Rostovtsev, L. G. Green, V. V. Fokin and K. B. Sharpless, *Angew. Chem., Int. Ed.*, 2002, **41**, 2596–2599.
29 P. Rejmanová, J. Kopeček, R. Duncan and J. B. Lloyd, *Biomaterials*, 1985, **6**, 45–48.
30 W. C. Chan and P. D. White, *Fmoc Solid-Phase Peptide Synthesis: A Practical Approach*, Oxford University Press, New York, 2000.
31 N. V. Tsarevsky, B. S. Sumerlin and K. Matyjaszewski, *Macromolecules*, 2005, **38**, 3558–3561.
32 R. Berg and B. F. Straub, *Beilstein J. Org. Chem.*, 2013, **9**, 2715–2750.
33 S. Binauld, F. Boisson, T. Hamaide, J. P. Pascault, E. Drockenmuller and E. Fleury, *J. Polym. Sci., Part A: Polym. Chem.*, 2008, **46**, 5506–5517.
34 V. Turk, B. Turk and D. Turk, *EMBO J.*, 2001, **20**, 4629–4633.
35 Y. Hashimoto, H. Kakegawa, Y. Narita, Y. Hachiya, T. Hayakawa, J. Kos, V. Turk and N. Katunuma, *Biochem. Biophys. Res. Commun.*, 2001, **283**, 334–339.
36 H. Appelqvist, P. Wäster, K. Kågedal and K. Öllinger, *J. Mol. Cell Biol.*, 2013, **5**, 214–226.
37 M. Azarkan, A. El Moussaoui, D. van Wuytswinkel, G. Dehon and Y. Looze, *J. Chromatogr. B: Biomed. Sci. Appl.*, 2003, **790**, 229–238.
38 N. Larson, J. Yang, A. Ray, D. L. Cheney, H. Ghandehari and J. Kopeček, *Int. J. Pharm.*, 2013, **454**, 435–443.